

Broadband moth-eye antireflection coatings on silicon

Chih-Hung Sun,¹ Peng Jiang,^{1,a)} and Bin Jiang²

¹Department of Chemical Engineering, University of Florida, Gainesville, Florida 32611, USA

²Department of Mathematics and Statistics, Portland State University, Portland, Oregon 97201, USA

(Received 19 December 2007; accepted 26 January 2008; published online 14 February 2008)

We report a bioinspired templating technique for fabricating broadband antireflection coatings that mimic antireflective moth eyes. Wafer-scale, subwavelength-structured nipple arrays are directly patterned on silicon using spin-coated silica colloidal monolayers as etching masks. The templated gratings exhibit excellent broadband antireflection properties and the normal-incidence specular reflection matches with the theoretical prediction using a rigorous coupled-wave analysis (RCWA) model. We further demonstrate that two common simulation methods, RCWA and thin-film multilayer models, generate almost identical prediction for the templated nipple arrays. This simple bottom-up technique is compatible with standard microfabrication, promising for reducing the manufacturing cost of crystalline silicon solar cells. © 2008 American Institute of Physics.

[DOI: 10.1063/1.2870080]

A solar cell converts absorbed photons into electrical charges.¹ Ideally, a solar cell should absorb all useful photons. However, more than 30% of incident light is reflected back from the surface of single-crystalline (SC) silicon solar cells which account for 36% of the 2004 production of photovoltaic panels.^{2–5} Antireflection coatings (ARCs) are therefore widely utilized to improve the conversion efficiencies of silicon solar cells.¹ Quarter-wavelength silicon nitride (SiN_x) films deposited by expensive plasma enhanced chemical vapor deposition (PECVD) are the industrial standard for ARCs on silicon substrates.² However, commercial SiN_x ARCs only exhibit low reflection at wavelengths around 600 nm and the reflection is increased to more than 10% for other wavelengths.^{1,4}

To achieve broadband ARCs, it is necessary to generate a graded refractive index layer that suppresses reflection over a broad range of wavelengths and angles of incidence.^{6–9} This is inspired by the subwavelength-structured corneas of nocturnal moths for the purpose of night camouflage.⁷ Top-down technologies, such as photolithography,¹⁰ electron-beam lithography,¹¹ nanoimprint lithography,¹² and interference lithography,^{3,6,13} are commonly used to generate subwavelength-structured ARCs. However, these expensive techniques require sophisticated equipment and are limited by either low resolution or small sample size. Bottom-up self-assembly provides a much simpler and cheaper alternative in creating submicrometer-scale periodic arrays.^{14–17} Unfortunately, traditional bottom-up technologies suffer from low throughput and incompatibility with standard microfabrication, limiting the mass production of practical ARCs.

We have recently developed a simple yet scalable templating technique for fabricating wafer-scale ARCs on SC silicon substrates.¹⁸ Subwavelength inverted pyramid arrays are anisotropically wet etched in SC silicon. Although this nonlithographic technique is much simpler and cheaper than PECVD deposition of SiN_x ARCs, the antireflective performance of the templated ARCs is not as good as the commercial coatings. The normal-incidence reflection is higher than

10% for most solar wavelengths due to the limited depth of the inverted pyramids.¹⁸ Additionally, the technique requires vacuum deposition of chromium which significantly increases the complexity and the cost for manufacturing ARCs on SC silicon solar cells.

Here, we report a bioinspired templating technique for fabricating broadband moth-eye ARCs on SC silicon substrates. The resulting subwavelength-structured ARCs exhibit superior broadband antireflective performance than commercial SiN_x coatings. The schematic illustration of the templating procedures for making wafer-scale silicon nipple arrays is shown in Fig. 1. Monolayer silica colloidal crystals with non-close-packed (ncp) structures are created by the established spin-coating technique.^{19,20} The ncp silica particles can be used as etching masks during a SF_6 reactive ion etching (RIE) process (40 mTorr chamber pressure, 26 SCCM (SCCM denotes cubic centimeter per minute at STP) SF_6 , 5 SCCM O_2 , 25 W) to pattern arrays of nipplelike structures directly on silicon wafers [test grade, n type, (100), Montco Silicon Technologies]. Under above RIE conditions, the etching selectivity between silicon and silica is more than 10:1.²¹ Templating silica spheres are finally removed by a hydrofluoric acid wash (2% aqueous solution) for 2 min.

Figure 2(a) shows a scanning electron microscope (SEM) image of a monolayer colloidal crystal consisting of 360 nm diameter silica spheres prepared by the spin-coating technique.²⁰ The long-range hexagonal arrangement and the ncp structure of silica particles are evident. Figure 2(b) shows a tilted SEM image of a sample after 9 min SF_6 etch. Due to the high etching selectivity between silicon and silica, the unprotected silicon is preferentially etched by reactive fluorine ions. The shrinkage of templating silica spheres is not significant. The RIE etching is isotropic, leading to the formation of nipplelike microstructures whose sizes and aspect ratios are determined by the templating silica sphere diameter and the RIE etching time. Figures 2(c) and 2(d) show tilted SEM images of silicon nipple arrays after 6 and 9 min RIE etching. The preservation of the hexagonal ordering and the interparticle distance of the original silica colloidal crystal are apparent for the templated nipple arrays. Subwavelength-scale nipples with aspect ratio as high as ~ 5.0 can be easily fabricated by this approach.

^{a)}Electronic mail: pjiang@che.ufl.edu.

**Spin-coated monolayer silica
colloidal crystal-polymer nanocomposite**

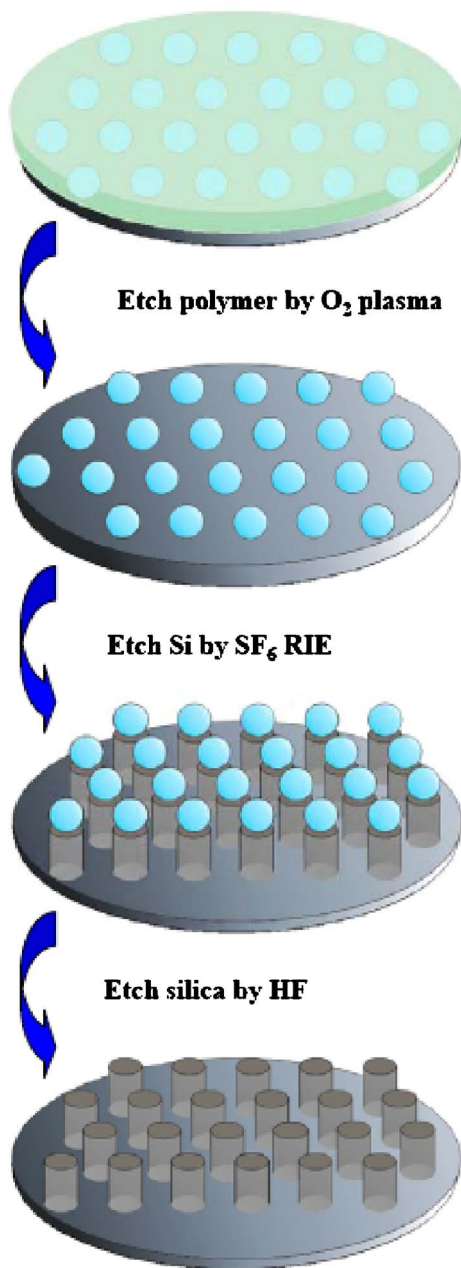


FIG. 1. (Color online) Schematic illustration of the templating procedures for fabricating moth-eye ARCs on silicon substrates.

The specular optical reflectivity of the templated silicon nipple arrays are evaluated using visible-near-IR reflectivity measurement at normal incidence.¹⁸ Figure 3 compares the normal-incidence reflection from a 15 min RIE-etched silicon nipple array sample, a bare SC silicon wafer, and a commercial SC silicon solar cell with PECVD-deposited SiN_x ARC (Plastecs, Webster, MA). The polished SC silicon wafer shows more than 35% reflection for wavelengths from 350 to 850 nm (black solid line), agreeing well with previous measurement.^{12,22} The Plastecs SC silicon solar cell exhibits distinctive bluish color caused by the SiN_x coating and presents the minimal reflection at around 700 nm (blue solid line). The templated nipple array shows excellent broadband antireflection property and the reflection is below 2.5% for a wide range of wavelengths (red solid line). The antireflective

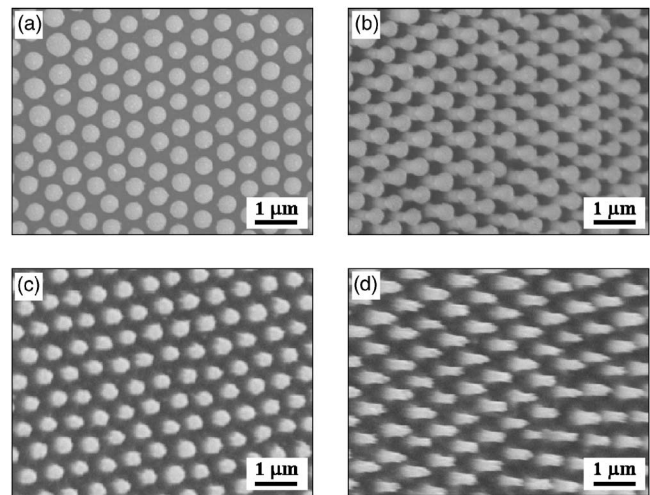


FIG. 2. (a) SEM image of a spin-coated monolayer non-close-packed colloidal crystal consisting of 360 nm silica spheres. (b) Tilted (20°) SEM image showing templating silica array and underneath silicon nipples etched by SF₆ RIE for 9 min. (c) Templated silicon nipple array after 6 min SF₆ etch. (d) Silicon nipples after 9 min SF₆ etch.

performance can be further optimized by using smaller silica particles as templates.⁷

The experimental reflection measurement is complemented by theoretical calculation using a rigorous coupled-wave analysis (RCWA) model.²³ A coordinate system is set up with z axis perpendicular to the nipple surface so that the array troughs are at $z=0$ and the nipple peaks at $z=h$. We divide the nipple arrays into $N=100$ horizontal layers with thickness h/N . The z -coordinate z^* and the radius r^* of each layer satisfy $r^*=r\sqrt{1-(z^*/h)}$, where $0\leq z^*\leq h$. The nipple lattice is assumed to be hexagonal and the distance between the centers of the neighboring troughs is defined as $\sqrt{2D}$, where D is the diameter of templating silica spheres.^{19,20} Therefore, the horizontal layer at level z^* contains a fraction

$f(z^*)$ of silicon with complex refractive index $\tilde{N}_{\text{Si}}=n+ik$ (n and k are optical constants obtained from literature)²⁴ and a

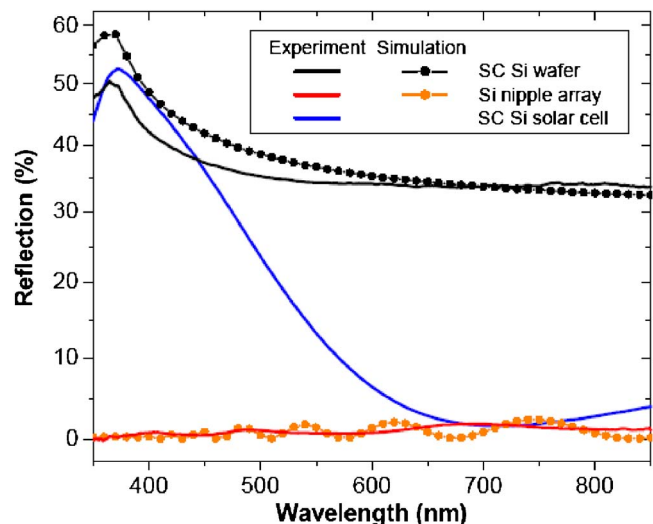


FIG. 3. (Color online) Experimental (solid) and RCWA-simulated (dotted) specular optical reflection at normal incidence for a flat single-crystalline silicon substrate (black lines), a commercial single-crystalline silicon solar cell with SiN_x ARC (blue line), and a 15 min etched silicon nipple array (red lines).

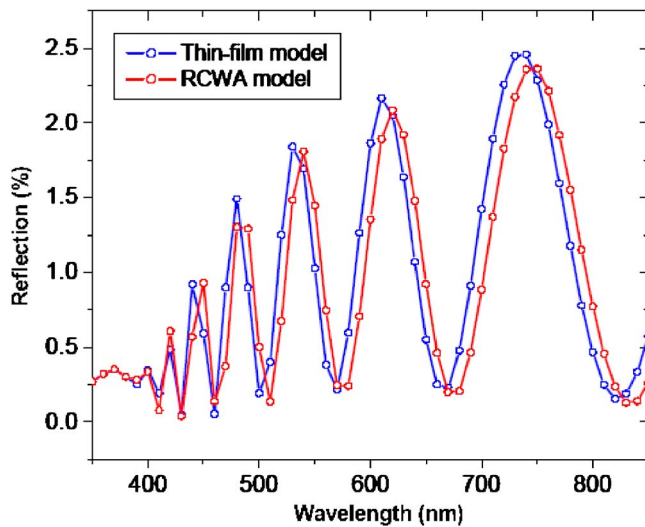


FIG. 4. (Color online) Comparison between the calculated optical reflection at normal incidence by the RCWA model (red) and the thin-film multilayer model (blue) for an array of nipples with 210 nm base radius and 800 nm height.

fraction $1-f(z^*)$ of air with refractive index $n_{\text{air}}=1$. The hexagonal structure of the nipple arrays leads to the formula $f(z^*)=[\pi(r^*)^2/\sqrt{3D^2}]$. Based on the effective medium theory,²⁵ the effective refractive index $n(z^*)$ of the layer at height z^* can be approximated by $n(z^*)=[f(z^*)N_{\text{Si}}^q + [1-f(z^*)]n_{\text{air}}^q]^{1/q}$, where $q=2/3$.^{7,25} We finally calculate the reflectance of the whole system by solving the Maxwell equation to express the electromagnetic (EM) field in each layer and then matching EM boundary conditions between neighboring layers for the determination of the reflectance of the system.²³

The dotted lines in Fig. 3 show the RCWA-simulated reflection from a bare silicon wafer and a subwavelength nipple array with base radius of 210 nm and height of 800 nm templated from 360 nm silica spheres. It is evident that the simulated results agree reasonably well with the experimental spectra for both samples, though both the peak position and the reflection magnitude match with the RCWA calculation for flat silicon, while only magnitude matches with theoretical prediction for periodic nipple arrays. This is due to the limitation of the RCWA modeling where each layer is assumed to have a uniform refractive index,²³ which is in fact a 2D periodic function at each layer. We further conduct optical modeling for the same subwavelength nipple array using another common simulation method—the thin-film multilayer (TFM) model.²⁵ The TFM model employs similar layer-slicing method as RCWA but a different matrix multiplication procedure to calculate the reflection from a

stack of thin layers. The simulation results obtained from both models are compared in Fig. 4. It is apparent that these two models generate almost identical results.

In summary, we have developed a simple yet scalable bottom-up approach for patterning subwavelength-structured nipple arrays directly on SC silicon substrates. The resulting gratings exhibit excellent broadband antireflection properties. The specular optical reflection from the templated moth-eye ARCs matches with theoretical predictions using RCWA and TFM models. These biomimetic coatings are of great technological importance in improving the conversion efficiencies of crystalline silicon solar cells.

This work was supported in part by the NSF under Grant No. CBET-0651780, the start-up funds from the University of Florida, and the UF Research Opportunity Incentive Seed Fund.

¹*Handbook of Photovoltaic Science and Engineering*, edited by A. Luque and S. Hegedus (Wiley, West Sussex, 2003), p. 268.

²P. Doshi, G. E. Jellison, and A. Rohatgi, *Appl. Opt.* **36**, 7826 (1997).

³A. Gombert, W. Glaubitt, K. Rose, J. Dreiholz, B. Blasi, A. Heinzl, D. Sporn, W. Doll, and V. Wittwer, *Thin Solid Films* **351**, 73 (1999).

⁴B. G. Prevo, E. W. Hon, and O. D. Velev, *J. Mater. Chem.* **17**, 791 (2007).

⁵*Thin Film Solar Cells: Fabrication, Characterization and Applications*, edited by J. Poortmans and V. Arkhipov (Wiley, West Sussex, 2006), p. xvii.

⁶B. Clapham and M. C. Hutley, *Nature (London)* **244**, 281 (1973).

⁷D. G. Stavenga, S. Foletti, G. Palasantzas, and K. Arikawa, *Proc. R. Soc. London, Ser. B* **273**, 661 (2006).

⁸C. Aydin, A. Zaslavsky, G. J. Sonek, and J. Goldstein, *Appl. Phys. Lett.* **80**, 2242 (2002).

⁹B. S. Thornton, *J. Opt. Soc. Am.* **65**, 267 (1975).

¹⁰C. Heine and R. H. Morf, *Appl. Opt.* **34**, 2476 (1995).

¹¹Y. Kanamori, E. Roy, and Y. Chen, *Microelectron. Eng.* **78–79**, 287 (2005).

¹²Z. N. Yu, H. Gao, W. Wu, H. X. Ge, and S. Y. Chou, *J. Vac. Sci. Technol. B* **21**, 2874 (2003).

¹³U. Schulz, *Appl. Opt.* **45**, 1608 (2006).

¹⁴J. Hiller, J. D. Mendelsohn, and M. F. Rubner, *Nat. Mater.* **1**, 59 (2002).

¹⁵N. H. Finkel, B. G. Prevo, O. D. Velev, and L. He, *Anal. Chem.* **77**, 1088 (2005).

¹⁶D. G. Choi, H. K. Yu, S. G. Jang, and S. M. Yang, *J. Am. Chem. Soc.* **126**, 7019 (2004).

¹⁷C. L. Haynes and R. P. Van Duyne, *J. Phys. Chem. B* **105**, 5599 (2001).

¹⁸C. H. Sun, W. L. Min, C. H. Lin, P. Jiang, and B. Jiang, *Appl. Phys. Lett.* **91**, 231105 (2007).

¹⁹P. Jiang and M. J. McFarland, *J. Am. Chem. Soc.* **126**, 13778 (2004).

²⁰P. Jiang, T. Prasad, M. J. McFarland, and V. L. Colvin, *Appl. Phys. Lett.* **89**, 011908 (2006).

²¹M. J. Madou, *Fundamentals of Microfabrication: The Science of Miniaturization*, 2nd ed. (CRC, Boca Raton, FL, 2002).

²²Y. Kanamori, K. Hane, H. Sai, and H. Yugami, *Appl. Phys. Lett.* **78**, 142 (2001).

²³M. G. Moharam, D. A. Pommert, E. B. Grann, and T. K. Gaylord, *J. Opt. Soc. Am. A* **12**, 1077 (1995).

²⁴M. A. Green and M. Keevers, *Prog. Photovoltaics* **3**, 189 (1995).

²⁵H. A. Macleod, *Thin-Film Optical Filters*, 3rd ed. (Institute of Physics, Bristol, 2001), p. 40.